Original Article

Role of Virtual Monoenergetic Images in the Assessment of Vessel Enhancement in Segmental Level in Third-Generation Dual-Source Dual-Energy CT Pulmonary Angiography—A Prospective Study

Vijayakumaran Ethiraju[1] Rajeshkumar Varatharajaperumal[1] Venkatesh Kasi Arunachalam[1]
Abdulla KuruVambath[1] Rajesh Shanmugam Punniyakotti[1] Sriman Rajasekaran[1] Pankaj Mehta[1]
Mathew Cherian[1]

[1] Department of Radiology, Kovai Medical Center and Hospital, Coimbatore, Tamil Nadu, India

Indian J Radiol Imaging

Address for correspondence Rajeshkumar Varatharajaperumal, DMRD, DNB, Department of Radiology, Kovai Medical Center and Hospital, Avanashi Road, Coimbatore 641014, Tamil Nadu, India (e-mail: Kumar2476rd@gmail.com).

Abstract

Introduction Pulmonary embolism is the third most common cause of cardiovascular death worldwide and imaging plays a pivotal role in establishing the diagnosis. Computed tomography pulmonary angiography (CTPA) scores over other modalities and is the current diagnostic investigation of choice. In this study, we assessed the main pulmonary artery and its corresponding segmental artery attenuation in reconstructed virtual monoenergetic (mono plus) images (VMI-MP) and linear blended images (spectral post processing, SPP) obtained from dual-energy CTPA. The values were compared using contrast-to-noise ratio (CNR) and signal-to-noise ratio (SNR).

Materials and Methods Forty patients (mean age group, 53.6 years; 26 females and 14 males) with segmental pulmonary thromboembolism were included in this prospective study. The patients underwent CTPA study using bolus tracking in the dual-source CT-SOMATOM Force, Siemens. Postcontrast datasets (90 kV, 150 kV, and SPP) were used to reconstruct the monoenergetic images using syngo.via software virtually. Comparison was done between bivariate samples using the paired sample t-test.

Results The mean Hounsfield unit (HU) artery in the left lung for VMI-MP and SPP images were 886.9 ± 242 and 356.8 ± 121.3 HU, respectively. Similarly, for the right lung, it was 868.3 ± 243.5 and 336.1 ± 105.5 HU, respectively. The mean attenuation of the arteries in MP images was higher and statistically significant (p-value <0.005). Likewise, the CNR) and SNR were found to have a statistically significant p-value (<0.005). An acceptable increase in image noise was seen in VMI as compared with SPP images.

Conclusion Low-keV VMIs perform more effectively than the conventional polyenergetic spectrum to evaluate vessel attenuation, which in turn increases thrombus detectability. The increased CNR in VMI enables improved lesion conspicuity.

Keywords
► dual-energy CT
► low keV
► segmental
► vessel attenuation
► VMI

Introduction

Pulmonary embolism (PE) is the third most common cause of cardiovascular death worldwide following stroke and myocardial infarction.[1] The vast majority of patients present with nonspecific complaints ranging from tachycardia to hemoptysis, and at times, they may be totally asymptomatic. Hence, a high index of suspicion is necessary to diagnose PE. Imaging plays a pivotal role in establishing the diagnosis of acute pulmonary thromboembolism (PTE). Ventilation (V) and perfusion (Q) scans are considered to surpass conventional radiography because of their higher sensitivity and specificity to detect PE. However, the PIOPED I (Prospective Investigation of Pulmonary Embolism Diagnosis) study by Vreim et al showed that 65% of the V/Q scans were nondiagnostic for PE.[2] Single-photon emission computed tomography (V/Q SPECT) provides better anatomical delineation over planar techniques for VQ imaging and improves diagnostic accuracy in the detection of PE. CT pulmonary angiography (CTPA) scores over other modalities and is the current diagnostic investigation of choice in suspected PE. The faster acquisition times and free availability with its higher diagnostic accuracy make it a far more advantageous investigation in the diagnosis of PE. All these factors paved the way for the widespread use of CTPA as the corner stone for the visualization of pulmonary arteries all the way to the subsegmental level. The key disadvantage that existed in the single source CT has been the visualization of the distal small branches of the pulmonary vessels. The recent innovations in CT include dual-energy and photon counting CT. The virtual monoenergetic images (VMI) is a subset of images generated from the dual-energy dataset. In low-keV VMI, the iodine containing structures showed increased attenuation compared with the rest of the areas. In the study done at our tertiary care center, we utilized this property of VMI and assessed the attenuation in the pulmonary arterial circulation and the image quality based on the contrast-to-noise ratio (CNR) and signal-to-noise ratio (SNR).

Materials and Methods

This prospective observational study was conducted in the department of radiology in a tertiary care hospital after obtaining ethical and scientific committee approval. The patients who presented to our hospital with chest pain, breathlessness, tachycardia, or desaturation had clinical suspicion of PTE underwent CTPA from December 2020 to June 2022 and were included in the study. A total of 40 patients were included in the study of which all of them had segmental PTE.

CT Technique

All the patients were subjected to CTPA study in the third-generation dual-source dual-energy CT (SOMATOM Force, Siemens). Automated tube-current modulation was activated in all examinations. Standard soft tissue kernels in post-contrast images were used to analyze the study. The patient

Table 1 CT parameters for acquisition of dual-energy datasets in SOMATOM Force, Siemens

Pitch	0.6
Tube A voltage	90 kV
Tube B voltage	150 kV
Tube A current	105 mAs
Tube B current	90 mAs

Abbreviation: CT, computed tomography.

was positioned supine with arms extended above the head. The patients were scanned in the craniocaudal direction with breath held in the maximal inspiratory effort. Ultravist 320 mg/mL (Bayer Schering Pharma, Berlin, Germany) was used and a volume of 1 mL/kg was injected for each study. The bolus tracking method was used in which phase I consists of 30 mL of saline with a flow rate of 4.5 mL/s and was injected using an automated dual syringe power injector through an 18 gauge intravenous access placed in the right median cubital/cephalic vein. This was followed by phase II consisting of contrast with a flow rate of 4.5 mL/s, and finally, phase III saline chase with 30 mL of saline at the same flow rate. Region of interest (ROI) was placed in the main pulmonary trunk and the scan was triggered when +100 Hounsfield unit (HU) was reached, with a delay of 4 seconds. Dual-energy datasets (90 and 150 keV) were obtained. Each patient had three sets of images (90 kV, 150 kV, and SPP) following contrast injection.

Dual-energy postcontrast study was obtained using the parameters as mentioned in ►**Table 1**.

After the completion of image acquisition, images were transferred to a dedicated workstation (syngo.via, Siemens) for further analysis. The dual-energy images obtained were post-processed to obtain the VMIs at 40 keV, in 1 mm slice thickness.

Evaluation of CT Findings

We had two subsets of images for each patient, which includes VMI (40 keV) and linear blended images. The vessel attenuation at the segmental level was calculated for all the segments of both lungs in both VMI and linear blended images, which are then extrapolated to the corresponding lobes/lungs. The bronchopulmonary segments were divided into 8 on the left side and 10 on the right side as per anatomical classifications. The vascular attenuation was measured by placing the circular ROIs with a minimum area of 1 mm^2 and repeated twice to obtain consistency for which the average of the two values was used. The HU of the muscle was obtained by placing the ROI in the pectoralis muscle with a minimum area of 1 cm^2. The image noise is defined as the standard deviation (SD) of the HU of muscle.

Quantitative Analysis

The CNR can be derived with the following equation:

$$CNR = HU \ (pulmonary\ artery) - HU\ (muscle)/image\ noise$$

Table 2 Demonstrating HU of arteries in VMI-MP and SPP for right and left lungs

	Mean	Number	SD
Left lung—HU artery (MP)	886.991	40	242.0557
Left lung—HU artery (SPP)	356.834	40	121.3978
Right lung—HU artery (MP)	868.388	40	243.5138
Right lung—HU artery (SPP)	336.179	40	105.5403

Abbreviations: HU, Hounsfield unit; MP, monoplus; SD, standard deviation; VMI, virtual monoenergetic image.

The SNR can be derived with the following equation:

$$\text{SNR} = \text{HU (pulmonary artery)/image noise}$$

Statistical Analysis

The data for VMI and linear blended images were collected in a Microsoft Excel sheet. The collected data were analyzed with IBM SPSS Statistics for Windows, Version 23.0 (Armonk, New York, United States: IBM Corp). To describe the data descriptive statistics, frequency analysis and percentage analysis were used for categorical variables, whereas mean and SD were used for continuous variables.

To find the significant difference between bivariate samples in paired groups, the paired sample *t*-test was used. In the above statistical tool, the probability value of 0.05 was considered a statistically significant level.

Results

A total of 40 patients who underwent CTPA in a dual-energy system for clinically indicated causes were included. The sample's mean age group was 53.6 ranging from 21 to 81 years. The majority of the patients were between 51 and 60 years which included 11 patients. Among the 40 patients included in the sample, the majority of them were females which comprised 26. The males constituted 14 out of 40 patients.

HU Arterial Attenuation of Lungs
The HU of segmental arteries was obtained which was then extrapolated to the corresponding right and left lungs. The

Table 4 Demonstrating HU of noise in MP and SPP for right and left lungs

	Mean	Number	SD
Left lung—HU noise (MP)	25.775	40	6.3548
Left lung—HU noise (SPP)	14.475	40	4.0191
Right lung—HU noise (MP)	25.550	40	6.3244
Right lung—HU noise (SPP)	14.325	40	3.9574

Abbreviations: HU, Hounsfield unit; MP, monoplus; SD, standard deviation.

mean HU value of the artery in the left lung for VMI monoplus (MP) images and linear blended (SPP) images were 886.9 ± 242 and 356.8 ± 121.3, respectively. Similarly, for the right lung, it was 868.3 ± 243.5 and 336.1 ± 105.5, respectively. The mean attenuation of the arteries in VMI-MP images was higher and statistically significant (*p*-value <0.005) (►**Tables 2** and **3**).

HU Noise of Lungs
The mean HU noise of the right lung was 25.7 ± 6.3 in MP and 14.4 ± 4 in SPP images, respectively. Similarly, in the left lung, it was 25.5 ± 6.3 in MP and 14.3 ± 3.9 in SPP. A significant increase in the noise was observed in MP images as compared with linear blended images (SPP). The decrease in energy caused an increase in the noise level of VMIs (►**Table 4**).

Contrast-to-Noise Ratio
By extrapolating the HU arteries obtained from the segmental arteries (8 segments in the left and 10 segments in the right lung) to the lobewise distribution following CNR was obtained (►**Fig. 1**).

Left Lung
The mean CNR for the upper lobe in MP and SPP were 33.8 ± 10.8 and 22.9 ± 8.9, respectively. Similarly, the mean CNR for the lower lobe was 31.7 ± 10.6 in MP and 21.5 ± 9.4 in SPP datasets (►**Tables 5** and **6**). The CNR was found to have a statistically significant *p*-value of less than 0.005 as mentioned in ►**Table 7**.

Right Lung
Similarly, a statistically significant *p*-value was obtained by calculating the CNR for all the lobes in both lungs as mentioned in ►**Tables 8** and **9**.

Table 3 Statistical comparison of arterial attenuation in MP and SPP for right and left lungs

HU artery (VMI-MP)–HU artery (SPP)	Paired differences					*t*-Value	Degree of freedom	*p*-Value
	Mean	Standard deviation	Standard error mean	95% confidence interval of the difference				
				Lower	Upper			
Left lung	530.156	140.2236	22.1713	485.3106	575.0019	23.912	39	0.0005
Right lung	532.208	162.3763	25.6740	480.2781	584.1391	20.730	39	0.0005

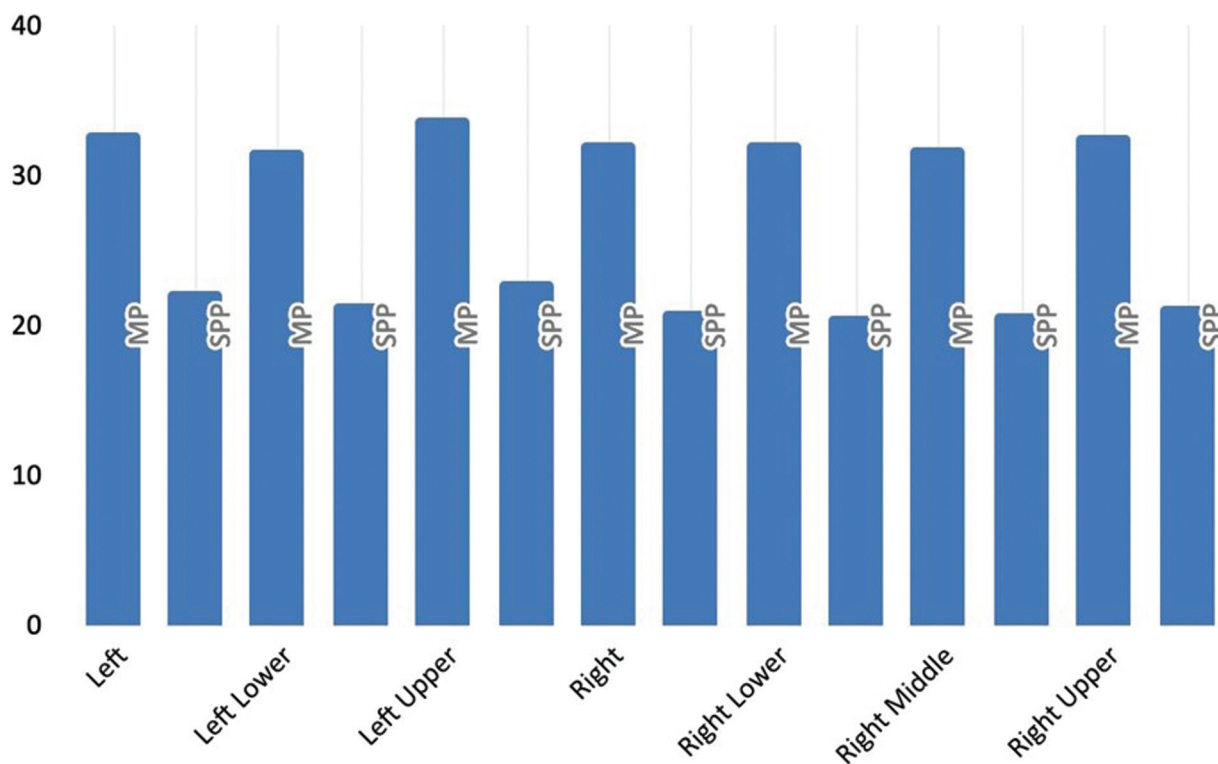Abbreviations: HU, Hounsfield unit; MP, monoplus; VMI, virtual monoenergetic image.

Fig. 1 Bar diagram showing mean CNR values in MP and SPP for all the lobes. CNR, contrast-to-noise ratio; MP, monoplus.

Table 5 Demonstrating CNR values of arteries in MP and SPP for left upper and lower lobes

Left lung	Mean	Number	SD
Upper lobe—CNR (MP)	33.894	40	10.8467
Upper lobe—CNR (SPP)	22.948	40	8.9607
Lower lobe—CNR (MP)	31.728	40	10.6772
Lower lobe—CNR (SPP)	21.530	40	9.4512

Abbreviations: CNR, contrast-to-noise ratio; MP, monoplus; SD, standard deviation.

Signal-to-Noise Ratio
By extrapolating the HU arteries obtained from the segmental arteries (8 segments in the left and 10 segments in the right lung) to the lobewise distribution following SNR was obtained (►**Fig. 2**).

Left Lung
The mean SNR for the upper lobe in MP and SPP were 36.6 ± 11 and 26.2 ± 9.2, respectively. Similarly, the mean SNR for the lower lobe was 34.4 ± 10.9 in MP and 24.8 ± 9.8 in SPP datasets. The SNR was found to have a statistically significant p-value of less than 0.005 as mentioned in ►**Tables 7** and **10**.

Right Lung
Similarly, a statistically significant p-value was obtained by calculating the SNR for all the lobes in both lungs as mentioned in ►**Tables 11** and **12**.

Discussion

Conventional CTPA images show decreased vessel attenuation in the distal pulmonary arteries, which could lead to less effective detection of PTE at this level. The attenuation in the distal arteries can be enhanced for optimal assessment by

Table 6 Statistical comparison of CNR values in MP and SPP for left upper and lower lobes

CNR (MP)–CNR (SPP)	Mean	Paired differences				t-Value	Degree of freedom	p-Value
		Standard deviation	Standard error mean	95% confidence interval of the difference				
				Lower	Upper			
Left upper lobe	10.9455	7.2965	1.1537	8.6120	13.2790	9.488	39	0.0005
Left lower lobe	10.1982	6.1393	.9707	8.2348	12.1617	10.506	39	0.0005

Abbreviations: CNR, contrast-to-noise ratio; MP, monoplus.

Table 7 Statistical significance of SNR values in left upper and lower lobes

SNR (MP)–SNR (SPP)	Mean	Paired differences				t-Value	Degree of freedom	p-Value
		Standard deviation	Standard error mean	95% Confidence interval of the difference				
				Lower	Upper			
Left upper lobe	10.3469	7.6892	1.2158	7.8878	12.8060	8.511	39	0.0005
Left lower lobe	9.5996	6.5387	1.0339	7.5085	11.6908	9.285	39	0.0005

Abbreviations: MP, monoplus; SNR, signal-to-noise ratio.

Table 8 Demonstrating CNR values of arteries in MP and SPP for right upper middle and lower lobes

Right lung	Mean	Number	SD
Upper lobe—CNR (MP)	32.683	40	12.3655
Upper lobe—CNR (SPP)	21.243	40	8.9702
Middle lobe—CNR (MP)	31.874	40	12.0122
Middle lobe—CNR (SPP)	20.824	40	9.1450
Lower lobe—CNR (MP)	32.683	40	12.3655
Lower lobe—CNR (SPP)	21.243	40	8.9702

Abbreviations: CNR, contrast-to-noise ratio; MP, monoplus; SD, standard deviation.

utilizing lower keV. It is based on the concept that lower energy approaching the K-edge value of iodine produces greater attenuation of the vessels. These low-keV VMIs are generated from a dual-energy dataset. The contrast of these VMI is high, but there is a slight increase in background noise. It is possible to increase the detectability of PTE in this subset of images because of an increase in attenuation of the density of vessels.

In our study, we reconstructed the VMI-MP at 40 keV and compared them with the standard linear blended images for assessing the vessel attenuation at different segmental arteries. The mean HU artery in the left lung for VMI-MP and linear blended (SPP) images were 886.9 ± 242 and 356.8 ± 121.3 HU, respectively (►**Fig. 3**). Similarly, for the right lung, it was 868.3 ± 243.5 and 336.1 ± 105.5 HU, respectively (►**Fig. 4**). The arteries in MP images had a higher mean attenuation which was statistically significant (p-value < 0.005).

By extrapolating the HU values for segmental arteries of the left upper lobe, the mean CNR in MP and SPP were 33.8 ± 10.8 and 22.9 ± 8.9, respectively. Likewise, the mean CNR for the lower lobe was 31.7 ± 10.6 in MP and 21.5 ± 9.4 in SPP datasets. The CNR was found to have a statistically significant p-value of less than 0.005. The CNR values obtained from MP images in the upper, middle, and lower lobes of the right side were statistically significant when compared with the SPP images. Despite the increase in background noise in VMI, the contrast attenuation was significantly higher, which had an impact on the overall image quality.

Delasalle et al showed conventional monoenergetic reconstructions at 60 keV provided adequate attenuation without significant artifacts in the majority of patients, with the highest SNR and CNR, the lowest level of subjective noise using a dual-source dual-energy approach at 80/140 kVp. In comparison to typical single-energy CTPA images, Delasalle et al demonstrated that virtual monoenergetic reconstructed image sets at 60 keV provide the greatest image quality both objectively (SNR and CNR) and subjectively (reduced artifacts and subjective noise).[3]

Past studies conducted by Matsumoto et al in 2011 evaluated the fast-switching dual-energy technique to assess the virtual monochromatic images for contrast assessment. They concluded that VMI images acquired at around 70 keV and reconstructed from split 80 and 140 kVp data displayed reduced image noise and greater CNR than typical 120 kV CT images.[4]

Recent studies by Yuan et al concluded that VMIs enhance the image quality of dual-energy CTPA with the 50 keV dataset offering the best outcomes for imaging of the

Table 9 Statistical significance of CNR values in right upper middle and lower lobes

CNR (MP)–CNR (SPP)	Mean	Paired differences				t-Value	Degree of freedom	p-Value
		Standard deviation	Standard error mean	95% confidence interval of the difference				
				Lower	Upper			
Right upper lobe	11.4400	8.6638	1.3699	8.6692	14.2108	8.351	39	0.0005
Right middle lobe	11.0496	7.8122	1.2352	8.5512	13.5481	8.946	39	0.0005
Right lower lobe	11.4400	8.6638	1.3699	8.6692	14.2108	8.351	39	0.0005

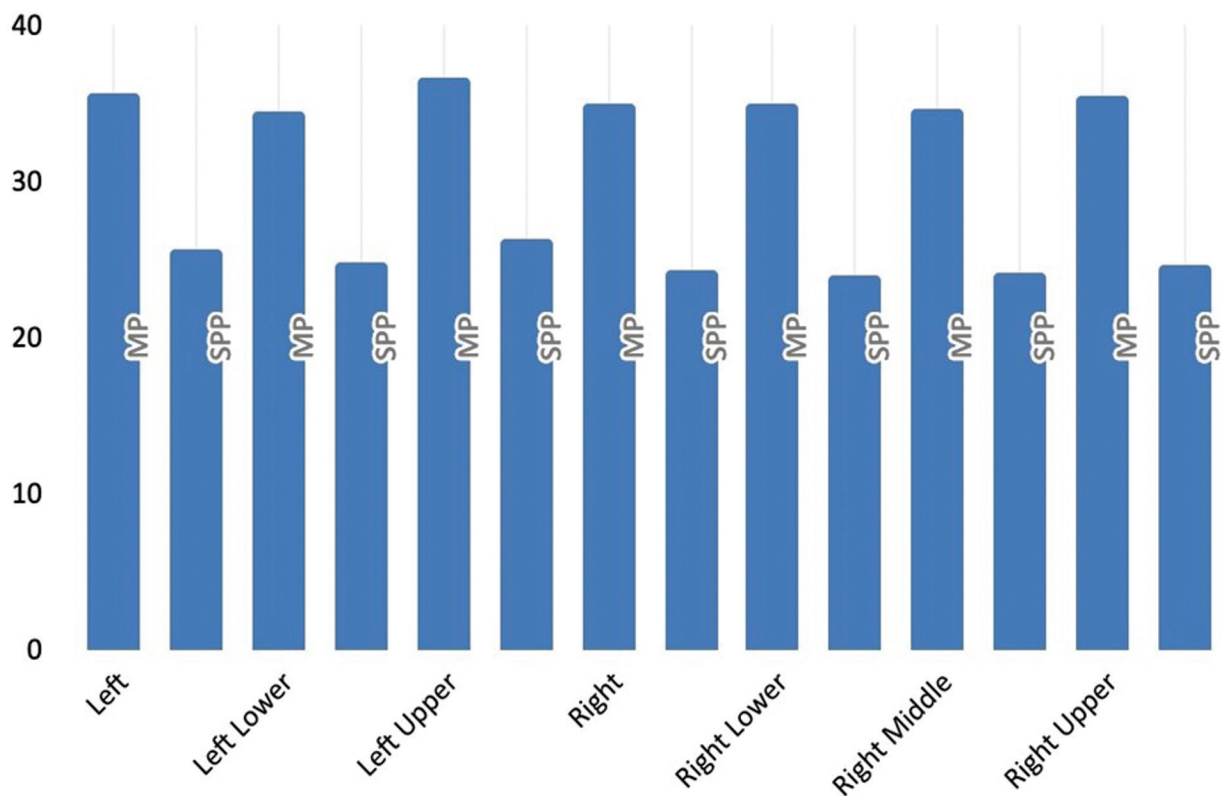Abbreviations: CNR, contrast-to-noise ratio; MP, monoplus.

Fig. 2 Bar diagram showing mean SNR values in MP and SPP for all the lobes. SNR, signal-to-noise ratio; MP, monoplus.

Table 10 Demonstrating SNR values of arteries in MP and SPP for left upper and lower lobes

Left lung	Mean	Number	SD
Upper lobe—SNR (MP)	36.638	40	11.0968
Upper lobe—SNR (SPP)	26.291	40	9.2658
Lower lobe—SNR (MP)	34.472	40	10.9139
Lower lobe—SNR (SPP)	24.873	40	9.8054

Abbreviations: MP, monoplus; SD, standard deviation; SNR, signal-to-noise ratio.

Table 11 Demonstrating SNR values of arteries in MP and SPP for right upper middle and lower lobes

Right lung	Mean	Number	SD
Upper lobe—SNR (MP)	35.428	40	12.5499
Upper lobe—SNR (SPP)	24.633	40	9.2524
Middle lobe—SNR (MP)	34.619	40	12.1218
Middle lobe—SNR (SPP)	24.214	40	9.4035
Lower lobe—SNR (MP)	34.939	40	10.2806
Lower lobe—SNR (SPP)	24.010	40	7.8846

Abbreviations: MP, monoplus; SD, standard deviation; SNR, signal-to-noise ratio.

pulmonary artery circulation, utilizing single-source dual-energy CT with rapid switching between 80 and 140 kVp.[5]

Assessment of image quality on dual-energy CTPA VMIs done by Dane et al proved that monoenergetic image data from dual-energy CTPA can deliver optimum image quality at 40 keV without considerable noise. The mean attenuation ranged from 914.83 HU for 40 keV images.[6] These results were quite similar to our study where the mean attenuation ranged from 878 ± 242 HU.

Meier et al performed a retrospective study to assess the contrast of VMI in dual-energy CTPA at lobar pulmonary branches.[7] MP 40 keV images showed a higher SNR and CNR in the pulmonary trunk and right lower lobe pulmonary artery compared with conventional images ($p < 0.001$).

Multiple studies have demonstrated that 40 keV monoenergetic datasets are optimal for reconstructing and assessing vascular attenuation for optimal imaging. Although the image noise was increased in monoenergetic images, a substantial increase in the HU value was observed even in the subsegmental arteries (►**Fig. 5**). Furthermore, numerous recent studies were performed in noise-optimized VMI-MP technique and found that quantitative image quality may be enhanced even further and exhibit the highest contrast attenuation.[8–12]

The SNR of the MP images during 40 keV reconstruction was compared with the SPP images in a similar manner. The SNR was found to have a statistically significant p-value of less than 0.005.

An acceptable increase in image noise was observed in 40 keV VMI-MP as compared with linear blended images in our study (►**Fig. 6**). The mean HU noise of the right lung was 25.7 ± 6.3 in MP and 14.4 ± 4 in linear blended (SPP) images, respectively. Similarly, in the left lung, mean HU was 25.5 ± 6.3 in MP and 14.3 ± 3.9 in SPP. In a study conducted

Table 12 Statistical significance of SNR values in right upper middle and lower lobes

SNR (MP)–SNR (SPP)	Mean	Paired differences				*t*-Value	Degree of freedom	*p*-Value
		Standard deviation	Standard error mean	95% confidence interval of the difference				
				Lower	Upper			
Right upper lobe	10.7953	9.0239	1.4268	7.9093	13.6813	7.566	39	0.0005
Right middle lobe	10.4049	8.1872	1.2945	7.7865	13.0233	8.038	39	0.0005
Right lower lobe	10.9289	7.8967	1.2486	8.4034	13.4544	8.753	39	0.0005

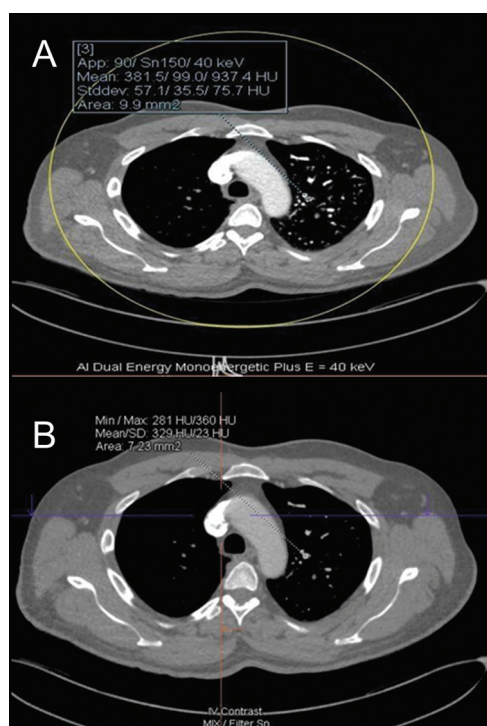Abbreviations: MP, monoplus; SNR, signal-to-noise ratio.

Fig. 3 Axial contrast-enhanced pulmonary angiography shows a higher attenuation value in 40 keV (MP) (**A**) as compared with the linear blended images (SPP) (**B**) measured left apicoposterior segmental branch. MP, monoplus.

by Leithner et al, when compared with linearly blended images, VMI reconstructions at 40 keV showed significantly higher attenuation in the pulmonary trunk (mean attenuation: 718.1 and 229.4 HU, respectively, $p = 0.001$), as well as significantly higher noise (average noise: 35.7 and 19.9 HU, respectively, $p = 0.001$).[13]

Beyond the various study designs that unite the aforementioned studies, a common finding is that low-keV VMIs perform more effectively than the conventional polyenergetic spectrum for the evaluation of vessel attenuation. This in turn reflects the detectability of thrombus. VMI's improved diagnostic performance is likely due to the increase in CNR, which allows for improved lesion conspicuity. In our study, low-keV images were able to detect the PE in some instances when it was not detected in blended images during the first evaluation. On the repeated review, it was visualized
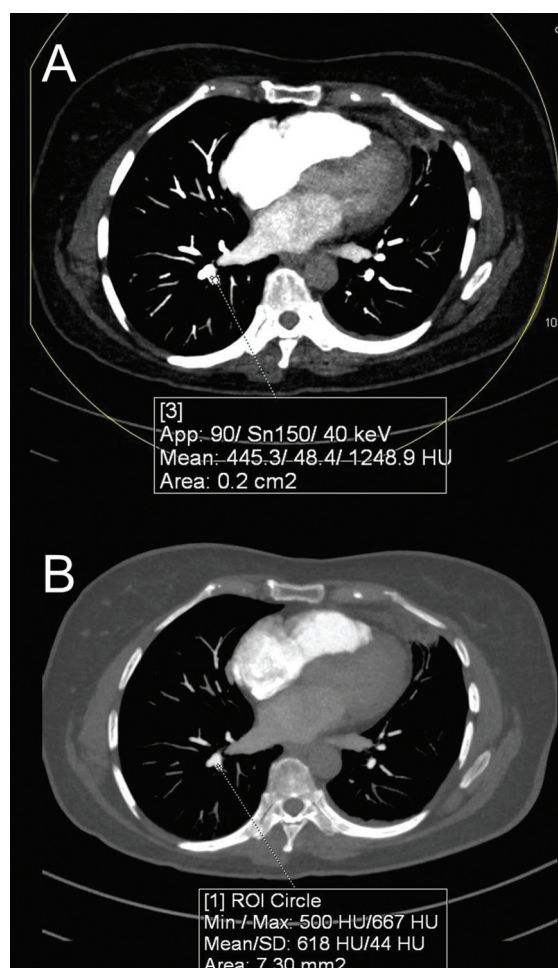

Fig. 4 Axial contrast-enhanced pulmonary angiography shows a higher attenuation value in 40 keV (MP) (**A**) as compared with the linear blended images (SPP) (**B**) measured right posterior basal segmental branch. MP, monoplus.

in linear blended images. Therefore, the diagnostic value of acute PE in doubtful or disregarded standard mixed images can be improved by using low-energy VMI+ images. In a study conducted by Leithner et al, where they assessed the diagnostic accuracy of VMI and iodine perfusion maps of dual-energy CTPA, they showed that when compared linear blended images in dual-energy CTPA with inadequate contrast attenuation, a reconstruction strategy using the 40-keV VMI-MP series and dual-energy CT-MP enhances reader
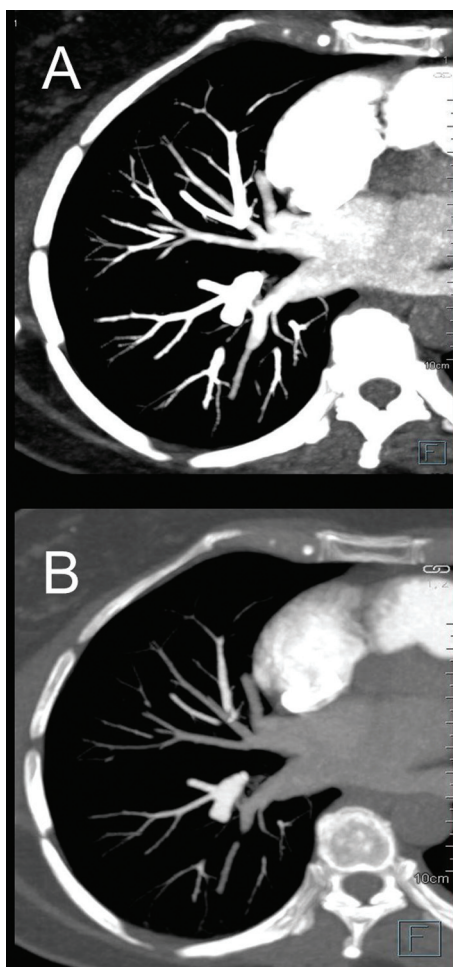
Fig. 5 Axial contrast-enhanced pulmonary angiography with maximal intensity projection shows optimal visualization of the segmental and subsegmental branches in 40 keV (MP) (**A**) as compared with the linear blended images (SPP) (**B**). MP, monoplus.

Fig. 6 Axial contrast-enhanced pulmonary angiography shows the measurement of noise in the form of the standard deviation of HU in the right pectoralis muscle. Significant increase in the background noise in the 40-keV (MP) images (**A**) was noted. However as compared to VMI images, the noise is lesser in Linear blended image (**B**). HU, Hounsfiled unit; MP, monoplus.

confidence and diagnostic accuracy for segmental PE identification. Therefore, if we are not able to detect PE in linear blended images, we can review low-keV images to confirm that it is truly negative for embolism. Although many studies have evaluated the role of VMI in assessing the density of pulmonary vessels, most of these studies have focused on analyzing larger vessels such as trunks and main pulmonary arteries.[7,13,14] To our knowledge, there are only very few studies that have been conducted to assess the pulmonary vascular attenuation at the segmental arterial level using the VMI-MP as we did.

Conclusion

To sum up, low-keV VMIs were superior to the conventional polyenergetic spectrum in assessing vessel attenuation, which in turn reveals the detectability of thrombus. Hence, utilizing VMI has the advantage of better CNR and SNR of the pulmonary arteries even at segmental levels, leading to an exceptional assessment with an acceptable increase in background noise. This can be recommended for optimal visualization of the segmental arteries for better detection of PTE.
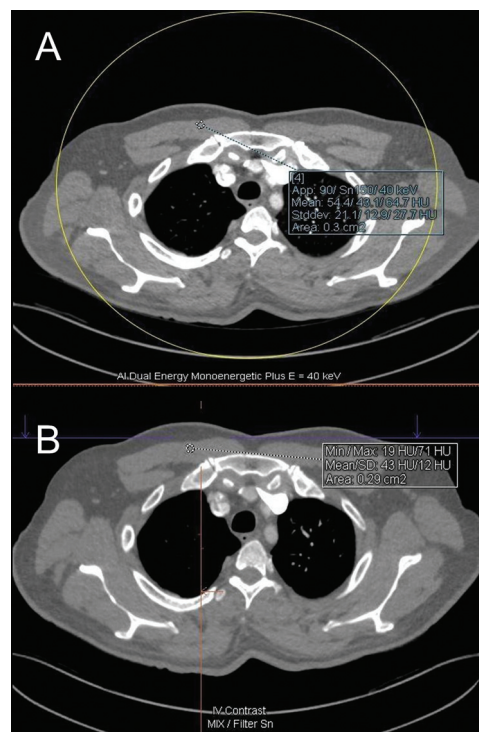
This prospective study patient group was rather limited to a small sample size; therefore, a larger scale study is required to support our findings. Currently, our results only apply to dual-source CT technology and cannot be immediately applied to dual-energy CT solutions by other vendors.

Conflict of Interest
None declared.

References

1 Goldhaber SZ, Bounameaux H. Pulmonary embolism and deep vein thrombosis. Lancet 2012;379(9828):1835–1846
2 Vreim CE, Saltzmann HA, Alavai A, et al. Value of the Ventilation/Perfusion Scan in Acute Pulmonary Embolism. Results of the Prospective Investigation of Pulmonary Embolism Diagnosis (PIOPED). The PIOPED investigators. JAMA 1990;263(20):2753–2759
3 Delesalle M-A, Pontana F, Duhamel A, et al. Spectral optimization of chest CT angiography with reduced iodine load: experience in 80 patients evaluated with dual-source, dual-energy CT. Radiology 2013;267(01):256–266
4 Matsumoto K, Jinzaki M, Tanami Y, Ueno A, Yamada M, Kuribayashi S. Virtual monochromatic spectral imaging with fast kilovoltage switching: improved image quality as compared with that obtained with conventional 120-kVp CT. Radiology 2011;259(01):257–262
5 Yuan R, Shuman WP, Earls JP, et al. Reduced iodine load at CT pulmonary angiography with dual-energy monochromatic imaging: comparison with standard CT pulmonary angiography–a prospective randomized trial. Radiology 2012;262(01):290–297

6 Dane B, Patel H, O'Donnell T, et al. Image quality on dual-energy CTPA virtual monoenergetic images: quantitative and qualitative assessment. Acad Radiol 2018;25(08):1075–1086

7 Meier A, Wurnig M, Desbiolles L, Leschka S, Frauenfelder T, Alkadhi H. Advanced virtual monoenergetic images: improving the contrast of dual-energy CT pulmonary angiography. Clin Radiol 2015;70(11):1244–1251

8 Grant KL, Flohr TG, Krauss B, Sedlmair M, Thomas C, Schmidt B. Assessment of an advanced image-based technique to calculate virtual monoenergetic computed tomographic images from a dual-energy examination to improve contrast-to-noise ratio in examinations using iodinated contrast media. Invest Radiol 2014; 49(09):586–592

9 Albrecht MH, Trommer J, Wichmann JL, et al. Comprehensive comparison of virtual monoenergetic and linearly blended reconstruction techniques in third-generation dual-source dual-energy computed tomography angiography of the thorax and abdomen. Invest Radiol 2016;51(09):582–590

10 Albrecht MH, Scholtz JE, Hüsers K, et al. Advanced image-based virtual monoenergetic dual- energy CT angiography of the abdomen: optimization of kiloelectron volt settings to improve image contrast. Eur Radiol 2016;26(06):1863–1870

11 Beeres M, Trommer J, Frellesen C, et al. Evaluation of different keV-settings in dual-energy CT angiography of the aorta using advanced image-based virtual monoenergetic imaging. Int J Cardiovasc Imaging 2016;32(01):137–144

12 Albrecht MH, Scholtz JE, Kraft J, et al. Assessment of an advanced monoenergetic reconstruction technique in dual-energy computed tomography of head and neck cancer. Eur Radiol 2015;25(08): 2493–2501

13 Leithner D, Wichmann JL, Vogl TJ, et al. Virtual monoenergetic imaging and iodine perfusion maps improve diagnostic accuracy of dual-energy computed tomography pulmonary angiography with suboptimal contrast attenuation. Invest Radiol 2017;52(11): 659–665

14 Murphy A, Cheng J, Pratap J, Redman R, Coucher J. Dual-energy computed tomography pulmonary angiography: comparison of vessel enhancement between linear blended and virtual monoenergetic reconstruction techniques. J Med Imaging Radiat Sci 2019;50(01):62–67